



FREQUENCY DOMAIN ARX MODEL AND MULTI-HARMONIC FRF ESTIMATORS FOR NON-LINEAR DYNAMIC SYSTEMS

D. E. ADAMS

*School of Mechanical Engineering, Purdue University, 1077 Ray W. Herrick Laboratories,
West Lafayette, IN 47907-1077, U.S.A. E-mail: deadams@purdue.edu*

(Received 11 January 2001, and in final form 7 August 2001)

Non-linear dynamic systems respond at frequencies other than the excitation frequency; however, standard frequency response function estimators for linear systems do not accommodate this harmonic distortion. A new multi-harmonic frequency response function estimator that utilizes discrete frequency models for non-linear systems is introduced here. The multi-harmonic estimator relates the frequency response at each frequency to the input and output spectra within a given frequency band in the same way that autoregressive exogenous input models relate inputs and outputs at particular samples in the time domain. Overdetermined, least-mean-squares calculations are used to minimize model error throughout a frequency band rather than at a single frequency as in the corresponding linear estimators. The resulting multi-harmonic frequency response function models are non-parametric (e.g., vary with amplitude) when linear functions are used and parametric when non-linear functions are used. A new sensitive indicator for experimentally characterizing non-linearity is introduced.

© 2002 Elsevier Science Ltd.

1. INTRODUCTION

Frequency response is central to experimental linear structural dynamics because it is minimal in the following sense: it relates inputs and outputs in the steady state at a single frequency only. Although this single-point relationship is sufficient for describing linear systems, a more inclusive relationship is required for non-linear systems because they respond at frequencies other than the excitation frequency. Common frequency response function (FRF) estimators, H_1 , H_2 , and H_v , do not accommodate this kind of harmonic distortion [1]. The goal of frequency domain analysis of non-linear systems is to describe how the harmonic amplitudes/phases of the response are related to one another and to the input amplitudes/phases. This research explores a new type of frequency response indicator for non-linear systems that accommodates multi-harmonic response behavior. The innovation is in the use of autoregressive exogenous input (ARX), or recursive, models in the *frequency domain*.

The most relevant previous research in the area of frequency response for non-linear structural dynamic systems includes the work of Volterra [2], Schetzen [3, 4], Storer and Tomlinson [5, 6], Bedrosian and Rice [7], Xu and Rice [8], Vinh and Liu [9], Worden [10], and others. These researchers have focused primarily on multi-dimensional convolution and frequency response as means for describing non-linear systems with sufficiently smooth non-linearities. Nikias and Petropulu [11] also provide a rigorous review of the theory of higher order spectra and Collis *et al.* [12] discuss some applications of these spectra.

In addition, Rice and Fitzpatrick [13], Bendat [14], Richardson and Singh [15, 16], and Adams and Allemang [17–20] have developed practical ways to describe non-linear multiple-input, multiple-output systems with smooth and/or discontinuous non-linearities using first order, nominal linear FRFs in conjunction with non-linear generating functions.

The research here directly exploits the notion of a discrete frequency model (DFM), which was introduced by Adams and Allemang [21]. This model relates the forced response of a given non-linear system to the input and the output at harmonics of the forcing frequency. The premise of that work is that the harmonic response at each frequency is correlated with both the input and the response at (potentially) all of the harmonics. This idea is used here to develop an approximate, more generalized characterization approach for non-linear systems subjected to broadband excitations, which produce frequency interactions and amplitude variations. Non-parametric and parametric ARX models will be used to estimate multi-harmonic FRFs that relate the broadband response at each frequency to the input at that frequency as well as the response at neighboring frequencies.

Sections 2.1–2.3 review higher order FRFs, the general form of a DFM, and time-domain ARX models. Then frequency domain ARX models are used in section 2.3 to describe frequency response relationships in simulations of a low order non-linear system. Section 2.4 analyzes the experimental data from a real-world non-linear system, and then conclusions and some discussion of future work are given in section 3.

2. MULTI-HARMONIC FRFs

2.1. HIGHER ORDER FREQUENCY RESPONSE

The basis of second and higher order frequency response analysis is the dynamic Taylor series, which is used to model input–output relationships in non-linear systems near nominal, or operating, points of interest. Figure 1 illustrates how different Volterra series expansions are used to model the system dynamics around two nominal points (i.e., * and **) that lie along a specific characteristic non-linear function, $F_n(A)$, where A is the characteristic co-ordinate. Each Volterra series expansion of the form,

$$y(t) = y_1(t) + y_2(t) + y_3(t) + \dots, \tag{1}$$

expresses the response, $y(t)$, of the (weakly) non-linear system to the input, $u(t)$, as a sum of the first ($y_1(t)$), second ($y_2(t)$), and higher order dynamic functions. Taylor series expansions

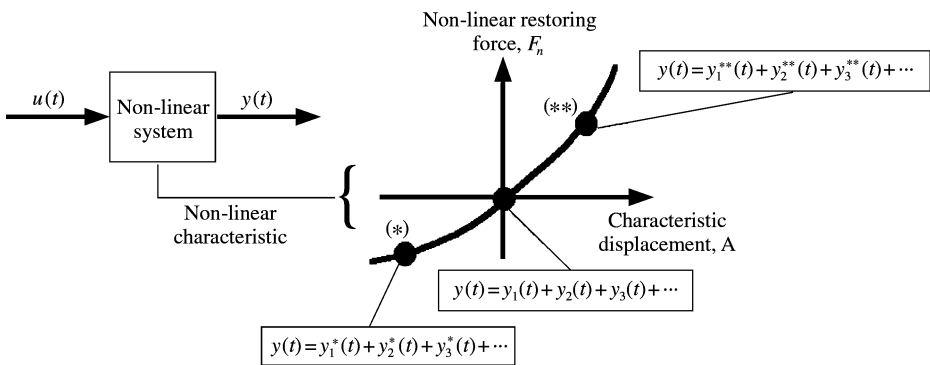


Figure 1. Piecewise non-linear Volterra functional series models near three nominal (operating) points of interest.

similarly describe differentiable functions as combinations of first, second, and higher order static functions.

Although the coefficients in Taylor series are static, the terms in the Volterra series are dynamic and are computed as follows:

$$y_1(t) = \int_{-\infty}^{+\infty} h_1(\tau)u(t - \tau) d\tau, \tag{2}$$

$$y_2(t) = \int_{-\infty}^{+\infty} \int_{-\infty}^{+\infty} h_2(\tau_1, \tau_2)u(t - \tau_1)u(t - \tau_2) d\tau_1 d\tau_2, \tag{3}$$

⋮

$$y_n(t) = \int_{-\infty}^{+\infty} \int_{-\infty}^{+\infty} \dots \int_{-\infty}^{+\infty} h_n(\tau_1, \tau_2, \dots, \tau_n)u(t - \tau_1)u(t - \tau_2) \dots u(t - \tau_n)d\tau_1 d\tau_2 \dots d\tau_n \tag{4}$$

where $h_n(\tau_1, \tau_2, \dots, \tau_n)$ is called the n th order Volterra kernel or impulse response function. The multi-dimensional Fourier transforms of the $h_n(\tau_1, \tau_2, \dots, \tau_n)$ are called higher-order FRFs:

$$H_n(\omega_1, \omega_2, \dots, \omega_n) = \int_{-\infty}^{+\infty} \int_{-\infty}^{+\infty} \dots \int_{-\infty}^{+\infty} h_n(\tau_1, \tau_2, \dots, \tau_n)e^{-j(\omega_1\tau_1 + \omega_2\tau_2 + \dots + \omega_n\tau_n)} d\tau_1 d\tau_2, \dots, d\tau_n. \tag{5}$$

Equation (5) can be used in conjunction with harmonic probing [9, 10] to obtain the frequency domain series corresponding to the time series in equation (1). For instance, if the non-linear Duffing oscillator,

$$m\ddot{y} + c\dot{y} + ky + \mu y^3 = u(t), \tag{6}$$

is driven by $u(t) = U_0 e^{j\omega_0 t}$ (a non-physical harmonic input), then the following response can be found:

$$\begin{aligned} y(t) &= H_1(\omega_0)U_0 e^{j\omega_0 t} + H_2(\omega_0, \omega_0)U_0^2 e^{j2\omega_0 t} + H_3(\omega_0, \omega_0, \omega_0)U_0^3 e^{j3\omega_0 t} + \dots \\ &= H_1(\omega_0)U_0 e^{j\omega_0 t} + 0e^{j2\omega_0 t} - \mu H_1^3(\omega_0)H_1(3\omega_0)U_0^3 e^{j3\omega_0 t} + \dots \\ &= H_1(\omega_0)U_0 e^{j\omega_0 t} - \mu(H_1(\omega_0)U_0)^3 H_1(3\omega_0)e^{j3\omega_0 t} + \dots, \end{aligned} \tag{7}$$

where $H_1(\omega) = 1/(k - m\omega^2 + j\omega c)$ and the $H_n(\omega_0, \omega_0, \dots, \omega_0)$ are higher order FRFs evaluated along the diagonal line $q_1 = q_2 = \dots = q_n = \omega_0$ in n -dimensional space. Therefore, the Fourier transform of $y(t)$ for a mono-frequency input can be written in the form

$$Y(\omega) = H_1(\omega)U(\omega) - \mu Y^3 \left(\frac{\omega}{3}\right) H_1(\omega) + 3\mu^2 Y^5 \left(\frac{\omega}{5}\right) H_1(\omega) + \dots \tag{8}$$

Note that this expression relates the response at a frequency ω to the mono-frequency input spectrum $U(\omega) = U_0 \delta(\omega - \omega_0)$ (where $\delta(\omega)$ is a delta function) and the output at harmonics of the excitation frequency; the equation is only true for this type of input. For example, the following sequence of steady state spectral response points can be generated using equation (8) for $u(t) = U_0 e^{j\omega_0 t}$:

$$Y(\omega_0) = H_1(\omega_0)U(\omega_0), \tag{9}$$

$$Y(3\omega_0) = -\mu Y^3(\omega_0)H_1(3\omega_0), \tag{10}$$

$$\begin{aligned}
 Y(5\omega_0) &= 3\mu^2 Y^5(\omega_0) H_1(5\omega_0), & (11) \\
 &\vdots = \vdots & (12)
 \end{aligned}$$

The equality constraints $U(3\omega_0) = U(5\omega_0) = \dots = 0$ and $Y(\omega_0/3) = Y(\omega_0/5) = \dots = 0$ were inserted into equation (8) to generate this sequence. These equalities only hold for an input of the form $U_0 e^{j\omega_0 t}$ in the absence of secondary resonances of the subharmonic or superharmonic type. The important feature in equation (8) is the direct dependence of forced superharmonic responses on the fundamental component, $Y_1(\omega_0) = H_1(\omega_0)U(\omega_0)$. The recursive nature of this result anticipates the new technique introduced in section 2.3.

Although the non-physical harmonic input does provide motivation for the work to follow, it does not capture the types of distortion that do occur in strongly forced non-linear systems. The physical harmonic probing input, $u(t) = U_0/2 \{e^{j\omega_0 t} + e^{-j\omega_0 t}\} = U_0 \cos(\omega_0 t)$, will capture these distortions. For this input, the steady state response of the Duffing oscillator is different but similar to equation (7),

$$\begin{aligned}
 y(t) &= H_1(\omega_0) \frac{U_0}{2} e^{j\omega_0 t} + H_1(-\omega_0) \frac{U_0}{2} e^{-j\omega_0 t} + \frac{3U_0^3}{4} H_3(\omega_0, \omega_0, -\omega_0) e^{j\omega_0 t} \\
 &+ \frac{3U_0^3}{4} H_3(\omega_0, -\omega_0, -\omega_0) e^{-j\omega_0 t} \\
 &+ \frac{U_0^3}{8} H_3(\omega_0, \omega_0, \omega_0) e^{j3\omega_0 t} + \frac{U_0^3}{8} H_3(-\omega_0, -\omega_0, -\omega_0) e^{-j3\omega_0 t} + \dots, \quad (13)
 \end{aligned}$$

where $H_3(\omega_1, \omega_2, \omega_3) = -\mu H_1(\omega_1) H_1(\omega_2) H_1(\omega_3) H_1(\omega_1 + \omega_2 + \omega_3)$. Note that the response at the (physical) excitation frequency, ω_0 , now has a component due to the third order FRF. Although this component renders the form in equation (8) inappropriate due to interactions between positive and negative frequency terms in $u(t)$, equation (8) can still be used to characterize the non-linearity as long as the excitation amplitude is not too large.

2.2. DISCRETE FREQUENCY MODELS (DFMs)

The DFM introduced in references [21, 22] is a generalization of equation (8) for single-input, single-output (SISO) systems subjected to multi-frequency inputs. More specifically, DFMs take the form

$$Y(\omega) \approx B(\omega)U(\omega) + \sum_{r,s \in \mathcal{R}_i} A_{r,s}(\omega) f_{r,s} \left(Y \left(\frac{p_r}{q_r} \omega \right), Y \left(\frac{p_s}{q_s} \omega \right) \right), \quad (14)$$

where r and s are contained in the set of real integers (\mathcal{R}_i), p_r, p_s, q_r , and q_s are integers indexed by r and s , $B(\omega)$ accounts for the nominal linear frequency response, and the $A_{r,s}(\omega)$ terms and $f_{r,s}(\cdot)$ functions accommodate superharmonic, subharmonic, and combination forced (not resonant) responses. Like equation (8), equation (14) indicates that the non-linear frequency response at a certain frequency depends on both the input at that frequency and the various response harmonics around that frequency. Figure 2 illustrates the DFM concept for a simple non-linear system.

Note that the model in equation (14) is valid for non-linear systems that exhibit roughly steady state responses to stationary inputs. This is because the model is based on the assumption of weak non-linearity [23]. For instance, systems which exhibit chaotic

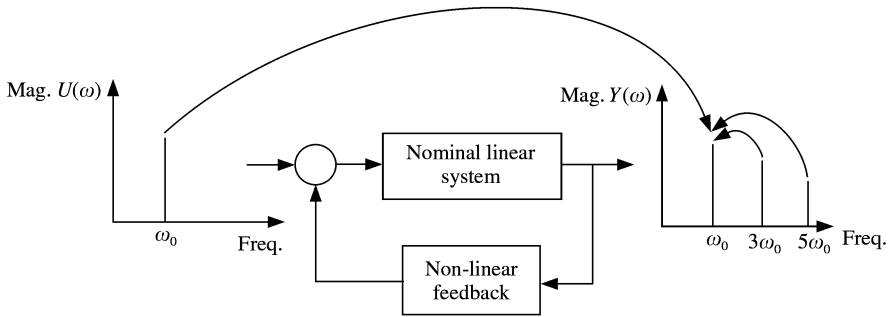


Figure 2. Illustration of internal feedback in a non-linear system with superharmonic response components. DFMs relate the response at the excitation frequency to the input and harmonic response components.

dynamics do not adhere to this model because periodic inputs to these kinds of systems often produce non-periodic, broadband responses [24].

2.3. TIME-DOMAIN ARX MODELS

ARX models (or infinite impulse response filters) [25, 26] have traditionally been used to describe dynamic systems as they evolve in time. Linear models of this type often take the following form for SISO systems:

$$y(k) = a_1 y(k - 1) + a_2 y(k - 2) + a_3 y(k - 3) + \dots + a_n y(k - n) + b_1 u(k - 1) + b_2 u(k - 2) + b_3 u(k - 3) + \dots + b_m u(k - m). \tag{15}$$

This equation expresses the output at the *k*th sample as a linear function of the previous *m* input samples and the previous *n* output samples. The *b_j* and *a_j* coefficients define the exogenous input portions and autoregressive portions, respectively, of the model. The order of the system is *n*, the largest delay in the autoregressive portion. Moving average terms can also be included as in ARMAX models by introducing an additional variable, *e(k)*, for instance, whereas non-linearity can be incorporated by permitting non-linear functions of the ARMA terms (i.e., NARMAX [27]).

In any typical experimental system identification approach using ARX models, equation (15) is used to search for the correlation between the input and output data, *u(t)* and *y(t)* with *t = kΔt* for integer *k > 0*. This correlation backward in time is what allows dynamic systems to evolve. Note that ARX models for causal systems by necessity have no ARX terms that look into the future (e.g., *a₋₁y(k + 1)*, *a₋₁ = 0*). The ARX coefficients are found by minimizing some objective function (e.g., sum of the squared error) associated with how well the model in equation (15) describes the measured data. For instance, if **y(k)** denotes an *N × 1* vector of output measurements leading up to sample *k*,

$$\mathbf{y}^T(k) = (y(k) \ y(k - 1) \dots \ y(k - N + 1))_{1 \times N}, \tag{16}$$

where *N* is the number of independent measurements, **u(k - 1)** denotes an *N × 1* vector of input measurements,

$$\mathbf{u}^T(k - 1) = (u(k - 1) \ u(k - 2) \ \dots \ u(k - N))_{1 \times N}, \tag{17}$$

and **p** denotes the (*m + n*) × 1 column vector of ARX coefficients,

$\mathbf{p} = (a_1 \ a_2 \ \dots \ a_n \ b_1 \ b_2 \ \dots \ b_m)^T$, then the error in the model for these samples is

$$\begin{aligned} \mathbf{e}(k) &= \mathbf{y}(k) \\ &\quad - [\mathbf{y}(k-1) \mathbf{y}(k-2) \ \dots \ \mathbf{y}(k-n) \mathbf{u}(k-1) \mathbf{u}(k-2) \ \dots \ \mathbf{u}(k-m)]_{N \times (m+n)} \mathbf{p} \\ &= \mathbf{A} \mathbf{p} \end{aligned} \tag{18}$$

and the optimum set of ARX coefficients (i.e., the ones that minimize the sum of the squared error, $\mathbf{e}(k) \cdot \mathbf{e}(k)$, for $N > m + n$) are given by the pseudo-inverse solution, $\hat{\mathbf{p}}$, to the overdetermined equation, $\mathbf{y}(k) = \mathbf{A} \mathbf{p}$:

$$\hat{\mathbf{p}} = \mathbf{A}^+ \mathbf{y}(k) = (\mathbf{A}^T \mathbf{A})^{-1} \mathbf{A}^T \mathbf{y}(k). \tag{19}$$

The pseudo-inverse of the measurement matrix is denoted with a $^+$ here. This solution forces the error, $e(k)$, from measurement to be uncorrelated (i.e., normal distribution), which is appropriate assuming that the model structure is adequate for capturing the dynamics in the measured data. This is the same procedure that will be used in what follows except that the proposed ARX model resides in the frequency domain rather than in the time domain. Note that selecting the model order, n , and the number of delays on the input, m , can often be the most challenging task in developing an accurate ARX model.

Although equation (15) is similar to equations (8) and (14), it differs in two essential ways. First, time-domain ARX models of causal non-linear systems only look backward in time, whereas frequency domain models look backward and forward in frequency. This dual-sided ARX nature of the frequency domain model, equation (14), can be attributed to an implicit time variance (multiple time scale) due to the non-linearity. In other words, the differential nature of the frequency domain analog of the ARX model in equation (15) produces implicit variations with time via the Fourier transform property, $\mathbf{F}[tf(t)] \leftrightarrow j\omega F(\omega)/d\omega$. Time-varying coefficients in the time domain thus result in differential terms in the frequency domain.

Second, time-domain ARX models of stationary causal non-linear systems have fixed coefficients, whereas the frequency domain models in equations (8) and (14) have coefficients that vary with frequency. In spite of this difference, it seems reasonable to present the proposed model in the ARX context because the coefficients at each frequency are fixed in the steady state.

2.4. FREQUENCY DOMAIN ARX MODELS

The proposed non-linear frequency response approach uses ARX models in the frequency domain to find FRF-like quantities, which can be used to characterize and identify non-linearity. The proposed ARX model is of the form

$$Y(k) = B(k)U(k) + \sum_{r,s \in \mathcal{R}_i} A_{r,s}(k) f_{r,s} \left(Y\left(\frac{p_r}{q_r} k\right), Y\left(\frac{p_s}{q_s} k\right) \right), \tag{20}$$

where k , r , s , $(p_r/q_r) k$, and $(p_s/q_s) k$ are contained in \mathcal{R}_i , k is simply the frequency counter, $\omega = k\Delta\omega$, and $B(k)$ and $A_{r,s}(k)$ are complex response coefficients. One term is included to account for the nominal linear dynamics, $B(k)U(k)$, and an autoregressive (AR) series is included to account for the non-linear multi-harmonic nature of the response spectrum, $Y(k\Delta\omega)$. The procedure used to find the coefficients in this model is identical to the one used in equation (19) to find the coefficients in the time-domain ARX model.

2.4.1. Zeroth order ARX FRF estimator

To illustrate the use, meaning, and implications of equation (20), consider the Duffing oscillator, equation (6), with the coefficients given in Table 1. The results to follow have been simulated using a fourth order, Dormand-Prince numerical integration scheme with a fixed size 0.01 s time step. 2^{17} (131, 072) length time histories were simulated for broadband random inputs with 1 and 5 N r.m.s. and 200 spectral averages with 60% overlap and a Hanning window were used to obtain FRF estimates. Standard H_1 FRF estimators, $\hat{H}_1(\omega) = G_{YU}(\omega)/G_{UU}(\omega)$, where $G_{YU}(\omega)$ and $G_{UU}(\omega)$ are cross-power and auto-power spectra [28], are calculated and compared with the multi-harmonic ARX FRF coefficients from equation (20).

The results from a standard pseudo-inverse spectral averaging procedure for the zeroth order frequency domain ARX model,

$$Y(k) = B(k)U(k), \tag{21}$$

are shown in Figure 3 along with the corresponding H_1 estimates for the linear ($\mu = 0 \text{ N/m}^3$) and non-linear ($\mu = 1e8 \text{ N/m}^3$) systems for 1 and 5 N r.m.s. inputs. The figure shows that the zeroth order ARX model is equivalent to the standard linear FRF (impedance) model and the exogenous coefficient, $B(k)$, is equivalent to the H_1 FRF

TABLE 1
System and simulation parameters for Duffing oscillator

Δt (s)	Nyquist Frequency (Hz)	m (kg)	c (N s/m)	k (N/m)	μ (N/m ³)
0.01	50	1	10	1000	1×10^8

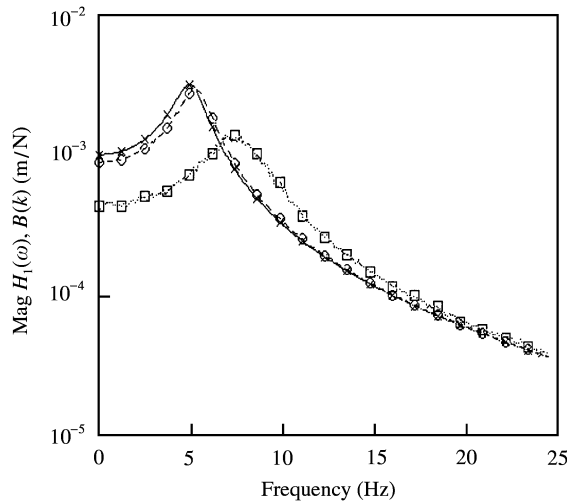


Figure 3. Linear FRF H_1 estimate and frequency domain ARX coefficients for zeroth order model (B): —, $\hat{H}_1(\omega)$ for linear systems; ---, $\hat{H}_1(\omega)$ for non-linear system with 1.0 N r.m.s. input;, $\hat{H}_1(\omega)$ for non-linear system with 5.0 N r.m.s. input; ×, $B(k)$ for linear system; ○, $B(k)$ for non-linear system with 1.0 N r.m.s. input; □, $B(k)$ for non-linear system with 5.0 N r.m.s. input. Note that the zeroth order estimators are equivalent to H_1 FRF estimators at a single frequency.

estimates. No multi-harmonic frequency response behavior is accommodated by this model.

2.4.2. Low order ARX model

The results of using the following first order frequency domain ARX model,

$$Y(k) = B(k)U(k) + A_1(k)Y(k - 1) + A_{-1}(k)Y(k + 1), \tag{22}$$

referred to as (B, A_1, A_{-1}) , to describe the Duffing oscillator are shown in Figures 4–6 along with the corresponding H_1 estimates for the linear ($\mu = 0 \text{ N/m}^3$) and non-linear ($\mu = 1e8 \text{ N/m}^3$) systems for 1 and 5 N r.m.s. inputs. The only frequency content in Figure 4 is at the modal frequency, $\omega_n = 2\pi \times 5 \text{ Hz}$, which is indicative of the linear frequency response behavior. In Figures 5 and 6, frequency content away from the nominal resonant frequency indicates that there are non-linear intra-frequency interactions that are only accounted for in the multi-harmonic ARX frequency response coefficients in equation (22). Also note that the frequency content in the ARX coefficients in Figure 6 is skewed towards higher frequencies because the input has a higher r.m.s. amplitude in this case.

In order to further interpret these results, recall that the ordinary coherence, $C(\omega)$, between an input, $U(\omega)$, and output, $Y(\omega)$, is given by

$$C(\omega) = \frac{|G_{YU}(\omega)|^2}{|G_{UU}(\omega)||G_{YY}(\omega)|}, \tag{23}$$

where $G_{YU}(\omega)$ is the cross-power spectrum and $G_{UU}(\omega)$ ($G_{YY}(\omega)$) is the input (output) auto-power spectrum [28]. Figure 7 shows \hat{H}_1 for the linear and non-linear system with a 1 N r.m.s. input, one minus the associated ARX coefficients (left), and the coherence function (right). Note that when $|A_1(k)|$ and $|A_{-1}(k)|$ are subtracted from unity, “enhanced” coherence functions are created. They are enhanced in the sense that they are more sensitive to non-linearity and other sources of correlated inputs (e.g., physically correlated inputs, signal processing leakage) than coherence. Figure 8 shows similar results for the 5 N r.m.s.

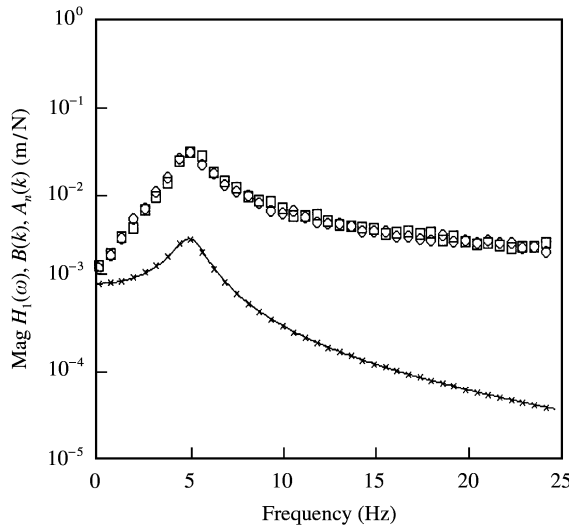


Figure 4. H_1 FRF estimates and frequency domain ARX coefficients for first order model (B, A_1, A_{-1}) . Linear system with: —, $\hat{H}_1(\omega)$; \times , $B(k)$; \circ , $A_1(k)$; \square , $A_{-1}(k)$. Note the recurring FRF ARX coefficient shape indicating no correlation with frequency in components of frequency response.

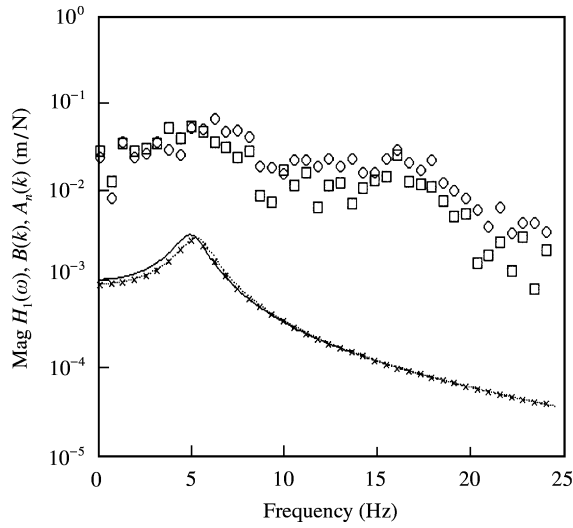


Figure 5. H_1 FRF estimates and frequency domain ARX coefficients for first order model (B, A_1, A_{-1}) : —, $\hat{H}_1(\omega)$ for linear system; ---, $\hat{H}_1(\omega)$ for non-linear system with 5 N r.m.s. input; \times , $B(k)$; \circ , $A_1(k)$; \square , $A_{-1}(k)$. Note the additional frequency content in the FRF ARX coefficients indicating correlation with frequency in frequency response.

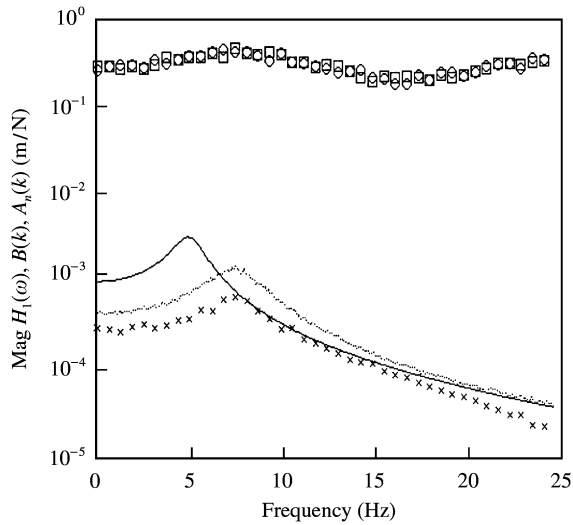


Figure 6. H_1 FRF estimates and frequency domain ARX coefficients for first order model (B, A_1, A_{-1}) : —, $\hat{H}_1(\omega)$ for linear system; ---, $\hat{H}_1(\omega)$ for non-linear system with 5 N r.m.s. input; \times , $B(k)$; \circ , $A_1(k)$; \square , $A_{-1}(k)$. Note the additional frequency content in the FRF ARX coefficients and the spectral location of these components.

input. The ARX coefficients are slightly more sensitive than coherence to leakage and system non-linearity in this case as well.

Since ordinary coherence functions and the proposed non-linear indicators, $1 - |A_1(k)|$ and $1 - |A_{-1}(k)|$, can be less than one even when the system is linear due to correlated inputs or signal processing errors (e.g., leakage), the results for a purely linear system must also be examined. Figure 9 shows (top) the frequency response function estimate, \hat{H}_1 , and the exogenous coefficient, $B(k)$, as well as (bottom) the coherence function and indicators,

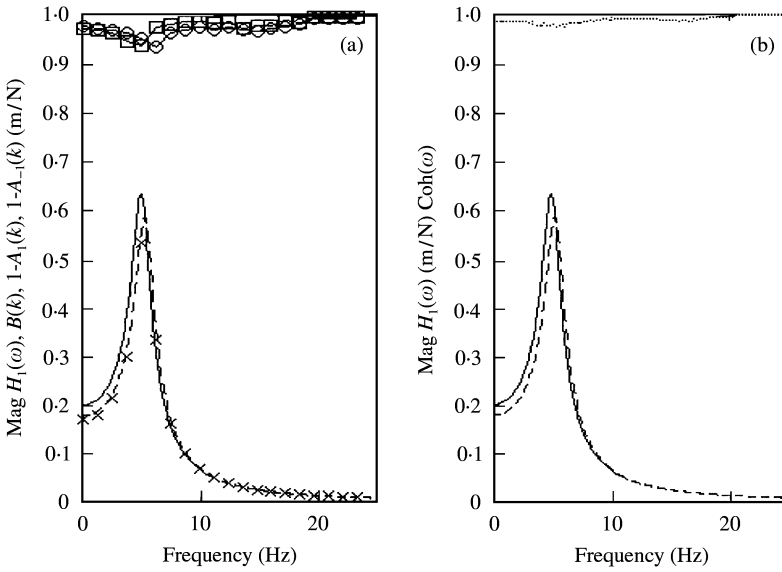


Figure 7. H_1 FRF estimate, frequency domain ARX coefficients (B , A_1 , A_{-1}) and ordinary coherence functions for non-linear system with 1 N r.m.s. input: (a) —, $\hat{H}_1(\omega)$; \times , $B(k)$; \circ , $1 - |A_1(k)|$; \square , $1 - |A_{-1}(k)|$; (b) ---, $\hat{H}_1(\omega)$; \cdots , $C(\omega)$.

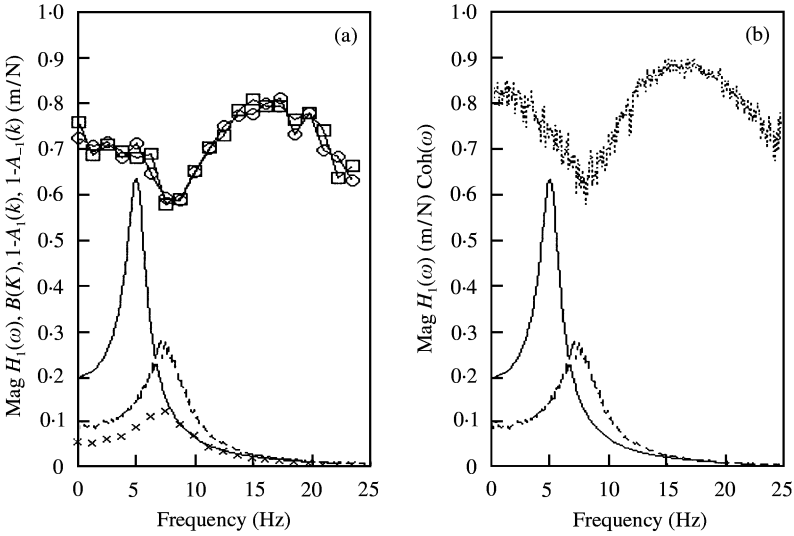


Figure 8. H_1 FRF estimate, frequency domain ARX coefficients (B , A_1 , A_{-1}), and ordinary coherence functions for non-linear system with 5 N r.m.s. input: (a) —, $\hat{H}_1(\omega)$; \times , $B(k)$; \circ , $1 - |A_1(k)|$; \square , $1 - |A_{-1}(k)|$; (b) ---, $\hat{H}_1(\omega)$; \cdots , $C(\omega)$.

$1 - |A_1(k)|$ and $1 - |A_{-1}(k)|$ (note the scale), for the linear system. The coherence only drops near the resonance because of leakage in the numerical Fourier transform; however, the proposed indicators are much more sensitive to the effects of leakage. This is because ARX indicators take into account biased errors that are correlated across a frequency range rather than coherence between an input and output at a single frequency.

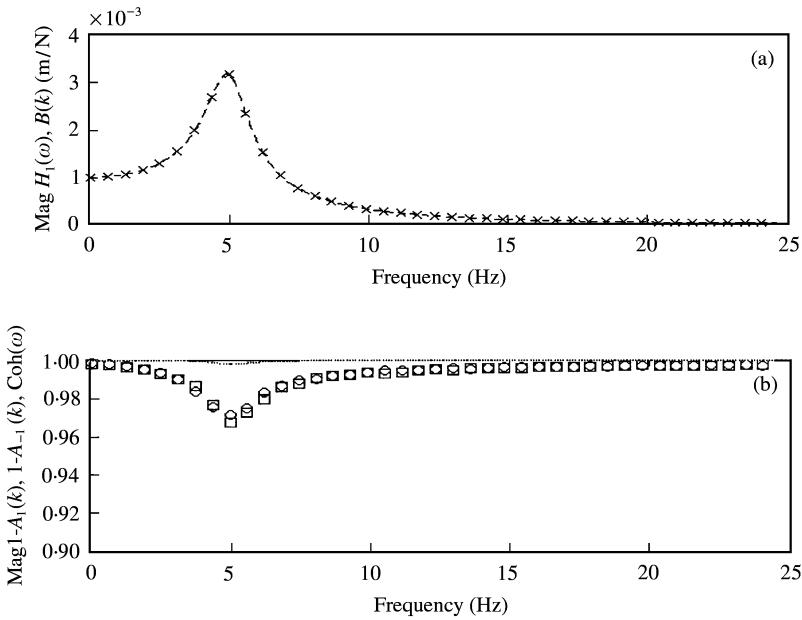


Figure 9. H_1 FRF estimate, frequency domain ARX coefficients $B(k)$, and ordinary coherence functions for a linear system with 1 N r.m.s. input: (a) ---, $\hat{H}_1(\omega)$; \times , $B(k)$; (b) \circ , $1 - |A_1(k)|$; \square , $1 - |A_{-1}(k)|$; \cdots , $C(\omega)$.

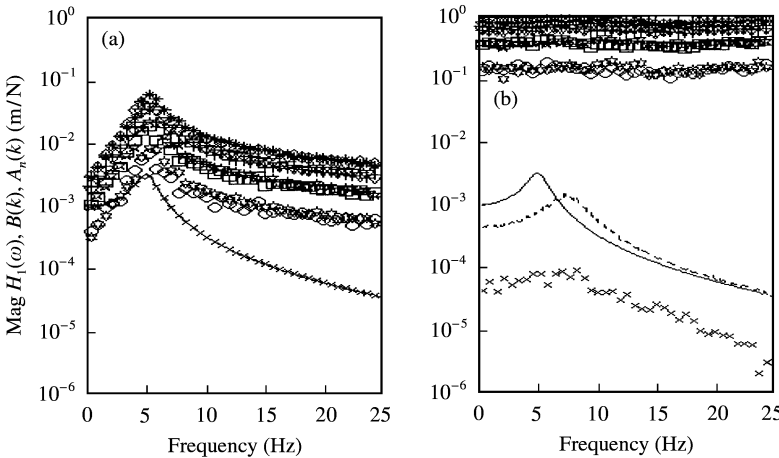


Figure 10. H_1 FRF estimates and ARX coefficients for fourth order model ($B, A_1, A_2, A_3, A_4, A_{-1}, A_{-2}, A_{-3}, A_{-4}$): (a) —, linear system $\hat{H}_1(\omega)$; \times , $B(k)$; \circ , $A_1(k)$; \square , $A_2(k)$; $+$, $A_3(k)$; \diamond , $A_4(k)$; $*$, $A_{-1}(k)$; Δ , $A_{-2}(k)$; \star , $A_{-3}(k)$; \blackstar , $A_{-4}(k)$, linear system; (b) —, linear system $\hat{H}_1(\omega)$; ---, non-linear system $\hat{H}_1(\omega)$ with 5 N r.m.s. input. Note the grouping of linear versus non-linear coefficients.

2.4.3. High order ARX model

The results of using the following fourth order frequency domain ARX model,

$$Y(k) = B(k)U(k) + A_4(k)Y(k - 4) + A_3(k)Y(k - 3) + A_2(k)Y(k - 2) + A_1(k)Y(k - 1) + A_{-4}(k)Y(k + 4) + A_{-3}(k)Y(k + 3) + A_{-2}(k)Y(k + 2) + A_{-1}(k)Y(k + 1), \quad (24)$$

referred to as ($B, A_1, A_2, A_3, A_4, A_{-1}, A_{-2}, A_{-3}, A_{-4}$), to describe the single degree-of-freedom non-linear Duffing oscillator are shown in Figure 10 along with the corresponding

H_1 estimates for the linear ($\mu = 0 \text{ N/m}^3$) and non-linear ($\mu = 1\text{e}8 \text{ N/m}^3$) systems for a 5 N r.m.s. input. Note that the ARX coefficients for the linear system always reflect the same linear input–output relationship; however, the coefficients other than $B(k)$ in the non-linear case assume large, nearly constant and distinct values. In effect, intra-frequency correlations dominate as the non-linearity becomes more severe.

2.4.4. Harmonic NARX models

All of the ARX models presented in sections 2.4.1–2.4.3 were linear and, therefore, non-parametric in nature. In other words, the coefficients varied as a function of the r.m.s. input amplitude. This is because for non-linear systems, non-linear functions must be used in order to capture variations with input and output amplitudes (refer to equation (20) or equation (8)). For example, the following expression might be used to capture these kinds of non-linear variations in the non-linear ARX (NARX) coefficients with amplitude:

$$Y(k) = B(k)U(k) + A_1(k)Y^3\left(\frac{k}{3}\right). \tag{25}$$

Figure 11 shows (right) two sets of zeroth order ARX coefficients ($B(k)$, magnitude and phase) for this model when two different r.m.s. input levels (1.0, 1.4 N) are used, and (left) the corresponding ARX coefficients for the linear first order model in equation (22). The true value of $H_1(\omega)$ is also given for reference. Note that the zeroth order AR coefficient, $B(k)$, is approximately the same for both input amplitudes, whereas the corresponding coefficient for the linear model is not the same. Thus, this model has captured some of the variations with input amplitude due to the non-linearity. As the input amplitude grows, however, even this NARX model will eventually show input dependence because it does not include non-linear terms that account for combination frequencies other than the third order. More

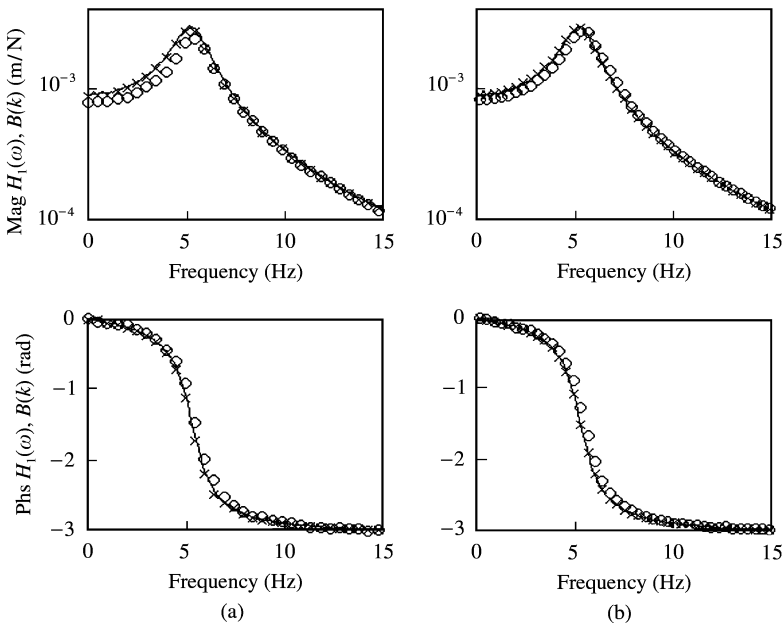


Figure 11. H_1 FRF estimate and frequency domain ARX coefficient $B(k)$ from NARX model: (a) —, $\hat{H}_1(\omega)$; \times , $B(k)$ for 1 N r.m.s. input; \circ , $B(k)$ for 1.4 N r.m.s. input for linear first order frequency domain ARX; (b) - - - -, $\hat{H}_1(\omega)$; \times , \circ , $B(k)$ for 1 N r.m.s. input; \circ , $B(k)$ for 1.4 N r.m.s. input for non-linear ARX model.

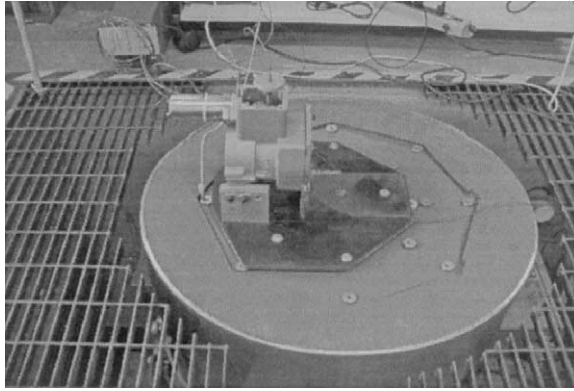


Figure 12. Experimental electrodynamic shaker and fixture set-up for examining the frequency domain ARX FRF coefficients.

sophisticated NARX models would have to be chosen in order to track the amplitude dependencies associated with these frequencies.

Figure 11 demonstrates an interesting point of application for these non-linear system identification frequency domain NARX models: even though the nominal linear FRF *magnitude* is not captured adequately by, for instance, the first order model in equation (22), the *phase* is well identified. Therefore, in applying frequency domain NARX or NARMAX models to non-linear systems, it is important to include separate criteria for phase comparisons between different models in order to assess good model fit in general.

2.5. EXPERIMENTAL FREQUENCY DOMAIN ARX MODELS

Figure 12 shows an experimental electrodynamic shaker set-up for examining the uses of frequency domain ARX models in non-linear structural dynamic system characterization and identification. A fixture and test specimen is shown with necessary instrumentation including four piezoelectric accelerometers and a 16 channel Agilent VXI data acquisition front-end with PC. Tests were conducted to characterize the internal dynamics of the electrodynamic shaker with and without the fixture and specimen installed. A broadband voltage input (200–2000 Hz) was supplied to the shaker and the accelerometer voltage on the shaker table was measured. Two hundred spectral averages with 55% overlap processing were used to estimate the H_1 FRF estimate, ARX model coefficients, and ordinary coherence functions (equation (23)).

Figure 13 shows the magnitudes of the H_1 FRF estimate and ARX coefficients for a first order model, (B, A_1, A_{-1}) . Note that the ARX coefficients A_1 and A_{-1} are small everywhere except below 200 Hz, near the shaker resonance at 1500 Hz, and as the frequency approaches 2000 Hz. The $B(k)$ coefficient is approximately equal to $\hat{H}_1(\omega)$ for all k except in these frequency ranges. Furthermore, these frequency ranges are precisely where the shaker is either not responding due to insufficient excitation or there is signal processing leakage. In other words, the two AR coefficients in the frequency domain ARX model seem to indicate coherence between the input and output (i.e., degree of linear correlation) and the MA coefficient indicates the nominal linear frequency responses (H_1). Figure 14 shows that when the magnitude of the AR coefficients are subtracted from one (left), they exhibit the same signature as the ordinary coherence function (right). Note that the ARX coefficients are more sensitive than coherence to leakage near 1500 Hz.

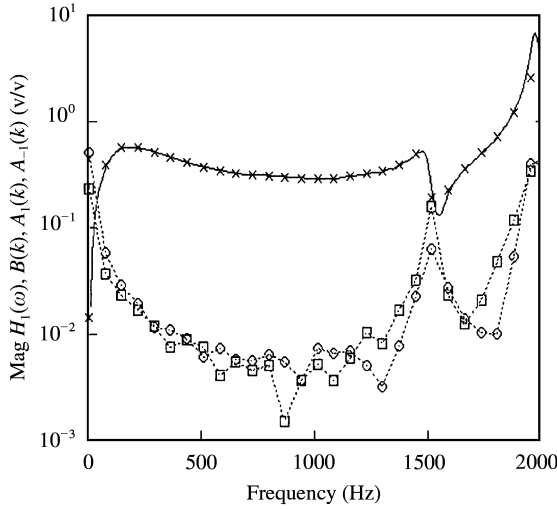


Figure 13. H_1 FRF estimate and frequency domain ARX coefficients for first order model (B , A_1 , A_{-1}) of electrodynamic shaker fixture: -----, $\hat{H}_1(\omega)$; \times , $B(k)$; \circ , $A_1(k)$; \square , $A_{-1}(k)$.

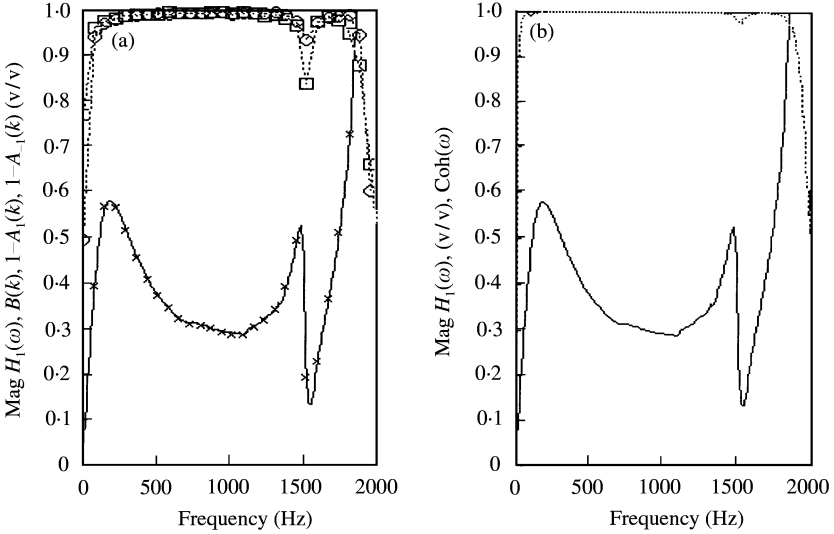


Figure 14. H_1 FRF estimate, frequency domain ARX coefficients (B , A_1 , A_{-1}), and ordinary coherence functions for electrodynamic shaker fixture: (a) -----, $\hat{H}_1(\omega)$; \times , $B(k)$; \circ , $1 - |A_1(k)|$; \square , $1 - |A_{-1}(k)|$; (b) -----, $\hat{H}_1(\omega)$; \cdots , $C(\omega)$.

3. CONCLUSIONS

Standard FRF estimators for linear systems capture input–output relationships at a single frequency only. Although this approach is adequate for linear system, non-linear systems exhibit correlation in frequency that can only be captured using multi-harmonic FRF estimators. Frequency domain ARX models, based on higher order FRFs and the concept of DFMs, can be used to estimate multi-harmonic frequency response relationships, which can then be used to characterize and potentially model forced non-linear systems. Each type of linear and non-linear ARX differencing term provides different FRF estimates that describe different types of non-linear behavior. Linear ARX

models are non-parametric in nature whereas non-linear ARX models are parametric, having been shown to capture some of the amplitude dependence common in non-linear input-output systems. ARX coefficients, especially those from higher order models, have also been shown to be more sensitive metrics of non-linearity than ordinary spectral coherence functions.

Weighted least squares is being explored as a means to develop other classes of FRFs for non-linear systems from ARX frequency domain models. In addition, methods for using the proposed model as a means for analysis are also being examined. Numerical issues associated with the broad experimental application of this technique are also being addressed.

ACKNOWLEDGMENT

In preparing this manuscript for publication, the author would like to acknowledge the insightful comments of anonymous reviewers of the journal.

REFERENCES

1. H. VOLD, J. CROWLEY and G. ROCKLIN 1985 *Proceedings of the International Modal Analysis Conference*, vol. 1, 272–278. A comparison of H_1 , H_2 , H_v frequency response functions.
2. V. VOLTERRA 1959 *Theory of Functionals and Integral Equations*. New York, NY: Dover Publications.
3. M. SCHETZEN 1989 *The Volterra and Wiener Theories of Nonlinear Systems*. Malabar: Krieger Publishing Company.
4. M. SCHETZEN 1981 *IEEE Proceedings* **69**, 1557–1573. Nonlinear system modeling based on the wiener theory.
5. D. M. STORER and G. R. TOMLINSON 1991 *Proceedings of the International Modal Analysis Conference*, vol. 2, 1206–1214. Higher order frequency response functions and their relation to practical structures.
6. D. M. STORER and G. R. TOMLINSON 1993 *Mechanical Systems and Signal Processing* **7**, 173–189. Recent developments in the measurement and interpretation of higher order transfer functions from non-linear structures.
7. E. BEDROSIAN and S. O. RICE 1971 *Proceedings of the IEEE* **59**, 1688–1707. The output properties of Volterra systems driven by harmonic and Gaussian inputs.
8. K. Q. XU and H. J. RICE 1998 *American Society of Mechanical Engineers Journal of Vibration and Acoustics* **120**, 125–130. On an innovative method of modeling general nonlinear mechanical systems. Part 1: theory and numerical simulations.
9. T. VINH and H. LIU 1992 *Identificazione Strutturale, October. Seriate, Bergamo*. Nonlinear structural dynamics by nonparametric method.
10. K. WORDEN 1992 *Identificazione Strutturale, October. Seriate, Bergamo*. Characterization of nonlinear systems using time data.
11. C. L. NIKIAS and A. P. PETROPULU 1993 *Higher-Order Spectra Analysis: A Nonlinear Signal Processing Framework*. Englewood Cliffs, NJ: PTR Prentice-Hall, Inc.
12. W. B. COLLIS, P. R. WHITE and J. K. HAMMOND 1998 *Mechanical Systems and Signal Processing* **12**, 375–394. Higher-order spectra: The bispectrum and trispectrum.
13. H. J. RICE and J. A. FITZPATRICK 1991 *Journal of Sound and Vibration* **149**, 397–411. A procedure for the identification of linear and non-linear multi-degree-of-freedom systems.
14. J. S. BENDAT 1998 *Nonlinear Systems Techniques and Applications*. New York, NY: John Wiley & Sons.
15. C. M. RICHARDS and R. SINGH 1998 *Journal of Sound and Vibration* **213**, 673–708. Identification of multi-degree-of-freedom non-linear systems under random excitations by the “reverse path” spectral method.
16. C. M. RICHARDS and R. SINGH 1998 *Journal of Sound and Vibration* **220**, 413–450. Feasibility of identifying non-linear vibratory systems consisting of unknown polynomial forms.

17. D. E. ADAMS and R. J. ALLEMANG 1999 *Journal of Sound and Vibration* **227**, 1083–1108. A new derivation of the frequency response function matrix for vibrating nonlinear systems.
18. D. E. ADAMS and R. J. ALLEMANG 1999 *Mechanical Systems and Signal Processing* **14**, 637–656. A frequency domain method for estimating the parameters of a nonlinear structural dynamic model through feedback.
19. D. E. ADAMS and R. J. ALLEMANG 2000 *Proceedings of the International Modal Analysis Conference San Antonio, TX*, vol. 1, 725–732. New spatial MDOF characterization and identification techniques for nonlinear systems.
20. D. E. ADAMS and R. J. ALLEMANG 2000 *Proceedings of the International Modal Analysis Conference San Antonio, TX*, vol. 1, 702–710. A superposition principle for nonlinear systems.
21. D. E. ADAMS and R. J. ALLEMANG 2000 *American Society of Mechanical Engineers Journal of Vibration and Acoustics* **123**, 98–103. Discrete frequency models: a new approach to temporal analysis.
22. D. E. ADAMS and R. J. ALLEMANG 2001 *International Journal of Non-Linear Mechanics* **36**, 1197–1211. Residual frequency autocorrelation as an indicator of nonlinearity.
23. A. H. NAYFEH and D. T. MOOK 1979 *Nonlinear Oscillations* New York, NY: John Wiley & Sons.
24. G. OTT 2000 *Chaotic Dynamics*. New York, NY: John Wiley & Sons.
25. R. W. HAMMING 1989 *Digital Filters*. Mineola, NY: Dover Publications, Inc.; third edition.
26. L. LJUNG 1987 *System Identification Theory for the User*. Englewood Cliffs, NJ: PTR Prentice-Hall.
27. S. CHEN and S. A. BILLINGS 1989 *International Journal of Control* **49**, 1012–1032. Representations of nonlinear systems: the NARMAX model.
28. J. S. BENDAT and A. G. PIERSOL 1980 *Engineering Applications of Correlation and Spectral Analysis* New York, NY: John Wiley & Sons.

APPENDIX A: NOMENCLATURE

FRF(s)	frequency response function(s)
ARX	autoregressive exogenous input
DFM(s)	discrete frequency model(s)
$y_1(t)$	n th order non-linear Volterra solution component
$h_n(\tau_1, \tau_2, \dots, \tau_n)$	n th order Volterra kernel
$H_n(\omega_1, \omega_2, \dots, \omega_n)$	Fourier transform n th order Volterra kernel
$u(t), y(t)$	input and output time histories
$U(\omega), Y(\omega)$	Fourier transforms of input and output respectively
$B(\omega)$	frequency response coefficient of $U(\omega)$ in discrete frequency model
$A_{r,s}(\omega)$	output spectrum coefficients in discrete frequency model
$f_{r,s}(\cdot)$	functions of harmonic elements of response spectra
$a_j(k)$	autoregressive (AR) coefficients in time-domain ARX model
$b_j(k)$	exogenous (X) coefficients in time-domain ARX model
n	maximum autoregressive delay
m	maximum exogenous input delay
$\mathbf{F}[f(t)]$	Fourier transform of $f(t)$
$Y(k)$	response spectrum evaluated at $k\Delta\omega$
$B(k)$	coefficient of $U(k)$ in frequency domain ARX model
\mathcal{R}_i	set of real integers
$A_{r,s}(k)$	frequency domain coefficients of autoregressive terms
$f_{r,s}$	functions of harmonic elements of response spectra
$\hat{H}_1(\omega)$	H_1 estimate of frequency response function
$G_{YU}(\omega)$	cross-power spectrum between input and output
$G_{UU}(\omega)$	auto-power spectrum of input
$C(\omega)$	ordinary coherence function between input $U(\omega)$ and output $Y(\omega)$
$ \cdot $	modulus of complex number